Appl. Phys. A (2015) 119:1423–1429
DOI 10.1007/s00339-015-9115-2

Applied Physics A
Materials Science & Processing

CrossMark

Experimental observations on the crystalline structures of $YAlO_3$ single crystal at high temperatures

Takahiro Inoue[1] · Takaaki Morimoto[1] · Yoshimichi Ohki[1,2]

Received: 3 September 2014 / Accepted: 18 March 2015 / Published online: 31 March 2015
© Springer-Verlag Berlin Heidelberg 2015

Abstract To understand the effects of thermal annealing on a high-permittivity gate insulating material $YAlO_3$, its single crystal was annealed at various high temperatures ranging from 900 to 1300 °C and was examined by various instrumental analyses such as X-ray diffraction, infrared absorption spectroscopy, laser confocal microscopy, and atomic force microscopy. As a result, it was clarified that the crystalline $YAlO_3$ takes at least three structures in a temperature range up to 1300 °C. Namely, it is perovskite below 1160 °C, at which the garnet structure starts to appear, while an unknown structure appears at 1250 °C. On the other hand, the sample surface also shows drastic changes if the temperature exceeds 1160 °C. Furthermore, many elliptical spots are induced after the annealing at 1200 or 1250 °C. Moreover, hydroxyl groups are generated at 1300 °C. It is desirable to take these structural changes into account in determining the annealing temperature of $YAlO_3$ for various industrial purposes such as the manufacture of semiconductor devices.

1 Introduction

Nowadays, power semiconductors are used more widely in various aspects of our daily life for various purposes. For example, power semiconductors used in power inverters, which are powerful tools for saving energy and electricity, are one of the key components in power electronic devices. In order to accelerate the use of power electronic devices more widely in various power apparatus, their operating voltages must be increased. In this regard, silicon carbide (SiC) is considered to be a promising candidate as a next-generation semiconducting material suitable for power semiconductors [1–3], because it has a wider band gap and can withstand much higher voltages than Si [1, 2, 4]. Furthermore, it has been reported that SiC power semiconductors are able to decrease losses in power substations [5]. Therefore, they can minimize energy consumption for power conversion significantly [1, 3, 5, 6]. As a typical recent example of their industrial applications, it has been reported that the use of SiC power semiconductors for power regression in an urban electric railway could reduce the energy consumption by about 30 % [7].

For gate insulating layers of Si-based semiconductor devices, SiO_2 has been used more widely. However, SiO_2 is not suitable for SiC-based semiconductor devices, since it cannot withstand high electric fields. The replacement of SiO_2 by a high-permittivity (high-k) dielectric can be a possible solution to this problem, since the layer thickness can be thickened [8, 9]. For this purpose, yttrium aluminate ($YAlO_3$) with a high-k ($\sim$15) [10] and a wide band-gap energy (E_g: 7.9 eV) [11] is a promising candidate. Another concern for SiC-based semiconductor devices is that high carrier mobility may not be attained due to the presence of a considerable amount of defects at the interfaces between the SiC and its dielectric [12]. Therefore, the high-k dielectric for SiC-based semiconductors must be free from defects. In this regard, a study on inherent or process-induced defects in high-k dielectrics is important.

Relating to the above, various annealing processes or treatments are necessary to manufacture semiconductor

✉ Takahiro Inoue
t.kiwoku@fuji.waseda.jp

Yoshimichi Ohki
yohki@waseda.jp

[1] Department of Electrical Engineering and Bioscience, Waseda University, Tokyo 169-8555, Japan

[2] Research Institute for Materials Science and Technology, Waseda University, Tokyo 169-8555, Japan

devices. Such treatments often induce electronic localized states and structural changes to dielectrics, which could degrade their insulating properties. From this viewpoint, we have been studying the effects of various treatments such as ion implantation, ultraviolet photon irradiation, and thermal annealing on various high-*k* dielectrics such as yttria-stabilized zirconia, lanthanum aluminate, and $YAlO_3$ [13–19]. In the present research, structural changes induced in $YAlO_3$ single-crystal samples by thermal annealing given in air at various high temperatures are examined.

2 Samples and experimental methods

Commercially available $YAlO_3$ (100) single crystals, grown by the Czochralski method by a German company Crystal GmbH, were examined in this study. The samples, in the shape of a plate with a thickness of 0.5 mm, were annealed in air at 1 atm using an electric furnace (KDF-1700, Denken) by raising the sample temperature from room temperature to various designated high temperatures between 900 and 1300 °C in 2 h. At each annealing temperature, the temperature was kept constant for 12 h.

After the sample was cooled naturally to room temperature from each annealing temperature, in-plane X-ray diffraction (XRD) patterns were obtained with Cu Kα X-rays using a Rigaku Rint-Ultima III, while Fourier transform infrared (FT-IR) spectra were obtained with both the transmission and attenuated total reflection (ATR) modes using a JASCO FT/IR-4200. Furthermore, the surface of the sample that had been used for the above-mentioned instrumental analyses was observed by the following four instrumental analyses. For two-dimensional observation in a square of several hundred micrometers, an optical microscope (VHX-2000, Keyence) and a laser confocal microscope (OLS4100, Shimadzu), which can weaken the effects of light scattering by focusing the laser beam, were used. In addition, an atomic force microscope (AFM, SPM-9700, Shimadzu), which can observe the surface in a square of several micrometers with a height resolution of nanometers, and a surface profilometer (Dektak 6M, Horiba), which measures the surface roughness along a straight line in a range of several hundred micrometers, were used. The surface profilometer has a height resolution of around 10 nm.

3 Results

In-plane XRD patterns measured before and after the annealing at various temperatures are shown in Fig. 1a. Note that only the patterns measured for the untreated sample and the samples annealed at 1200, 1250, and 1300 °C are shown to make the differences clear, although the annealing had also been done at 900, 1100, and 1160 °C.

The XRD peak at $2\theta = 34.6°$ appearing in the untreated sample is due to the perovskite $YAlO_3$ [20]. After the annealing at 1160 or 1200 °C, the intensity of the peak at 34.6° becomes weak, and it disappears at 1250 °C. In accordance with this decrease in the 34.6° peak, three new peaks appear at 33.6°, 32.6°, and 25.9°. While the peak at 33.6° is due to YAG (=$Y_3Al_5O_{12}$) [20], the one at 25.9° is attributable to Al_2O_3 [21]. However, the origin of the peak at 32.6° is unknown.

Figure 1b shows the annealing temperature dependence of each peak, normalized by the intensity of the peak at 34.6° before the annealing. Here, the intensities of the peaks after the annealing at 900, 1100, and 1160 °C that were omitted in Fig. 1a are also shown. While one of the three new peaks at 33.6°, which is rather strong, appears at

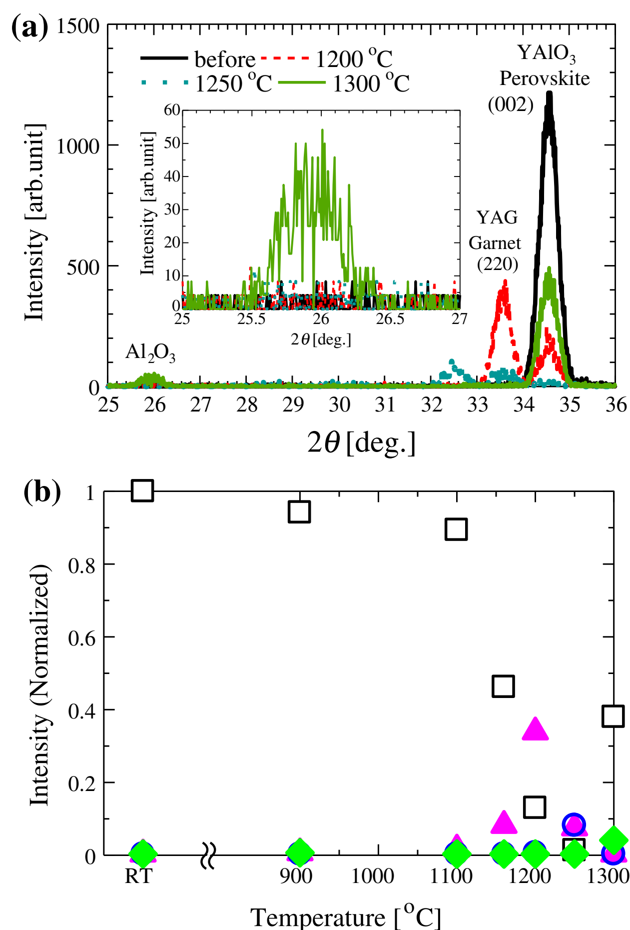

Fig. 1 **a** Effects of the thermal annealing at various temperatures on the in-plane XRD pattern of $YAlO_3$. The patterns at around 25.9° are enlarged in the *inset*. **b** Changes in the diffraction peak heights at 34.6° (*open square*), 33.6° (*filled triangle*), 32.6° (*open circle*), and 25.9° (*filled diamond*), normalized by the height of the 34.6° peak before the annealing. The *symbols* on the abscissa that cannot be seen are hidden by some others

1160 °C and becomes the maximum at 1200 °C, it becomes smaller at 1250 °C and disappears at 1300 °C. Concurrently with the behavior of the 33.6° peak, the peak at 34.6° that disappeared at 1250 °C re-appears again at 1300 °C. The two other peaks at 32.6° and 25.9° are very weak, and they appear only after the annealing at 1250 and 1300 °C, respectively.

The FT-IR spectra measured after the annealing at different temperatures are shown in Figs. 2 and 3. The spectra taken in the transmission mode shown in Fig. 2 do not provide meaningful information, apparently due to the thick sample thicknesses. Therefore, we mainly mention the ATR spectra shown in Fig. 3. Note that a clear peak seen in some samples in a range from 2300 to 2400 cm^{-1} in Fig. 3a is due to CO_2 gas remaining in the spectrometer. Besides this peak, an absorption peak is seen at around 655 cm^{-1} as shown in Fig. 3b. It has been reported that several absorption peaks, which are attributable to vibrations of bonds between metal and oxygen, namely either between Y and O or between Al and O, appear in $YAlO_3$ [22] and YAG [20] in a range from 300 to 800 cm^{-1}. The Ref. [20] assigned the vibrations due to Al–O in YAG to peaks at 791 and 692 cm^{-1}, and those due to Y–O to 727, 568, and 463 cm^{-1}. It is true that the wavenumber range of the FT-IR spectrum reported in [22] for $YAlO_3$ is too wide to judge whether the present absorption is the same as the one reported. Moreover, [22] did not mention the precise peak positions. However, these reports mentioned above together with the fact that the absorption at 655 cm^{-1} appears clearly before the thermal annealing seem to be enough for the assignment of the metal–oxygen vibration in $YAlO_3$ as the origin of the 655-cm^{-1} absorption.

After the annealing at 1200 °C, an IR-ATR peak appears at around 635 cm^{-1}. This peak may not be new, but a branch of the above-mentioned metal–oxygen vibration. Whether it is the case or not, it indicates the appearance of a crystal structure different from $YAlO_3$. Although the 635-cm^{-1} peak is also observable after the annealing at 1250 °C (not shown), it disappears after the annealing at 1300 °C. This temperature dependence of appearance and disappearance of the 635-cm^{-1} peak is quite similar to that of the 33.6° diffraction shown in Fig. 1b, which is attributed to YAG. Therefore, the 635-cm^{-1} peak originates in YAG.

Furthermore, only after the annealing at 1300 °C, three sharp ATR peaks appear in a range from 1000 to 1130 cm^{-1}. It has been reported that absorption appears in Al_2O_3 at 1080 cm^{-1} due to vibrations of Al–O–H [23]. Furthermore, it has also been reported that $Al(OH)_3$ shows absorption at around 1100 cm^{-1} [24]. Therefore, the three peaks are attributable to vibrations of bonds in a new structure induced by the thermal annealing at 1300 °C, which presumably contains OH. Since the three peaks are not observable in the IR spectra measured in the transmission mode as shown in Fig. 2c, the new structure was induced only in the surface layer of the sample.

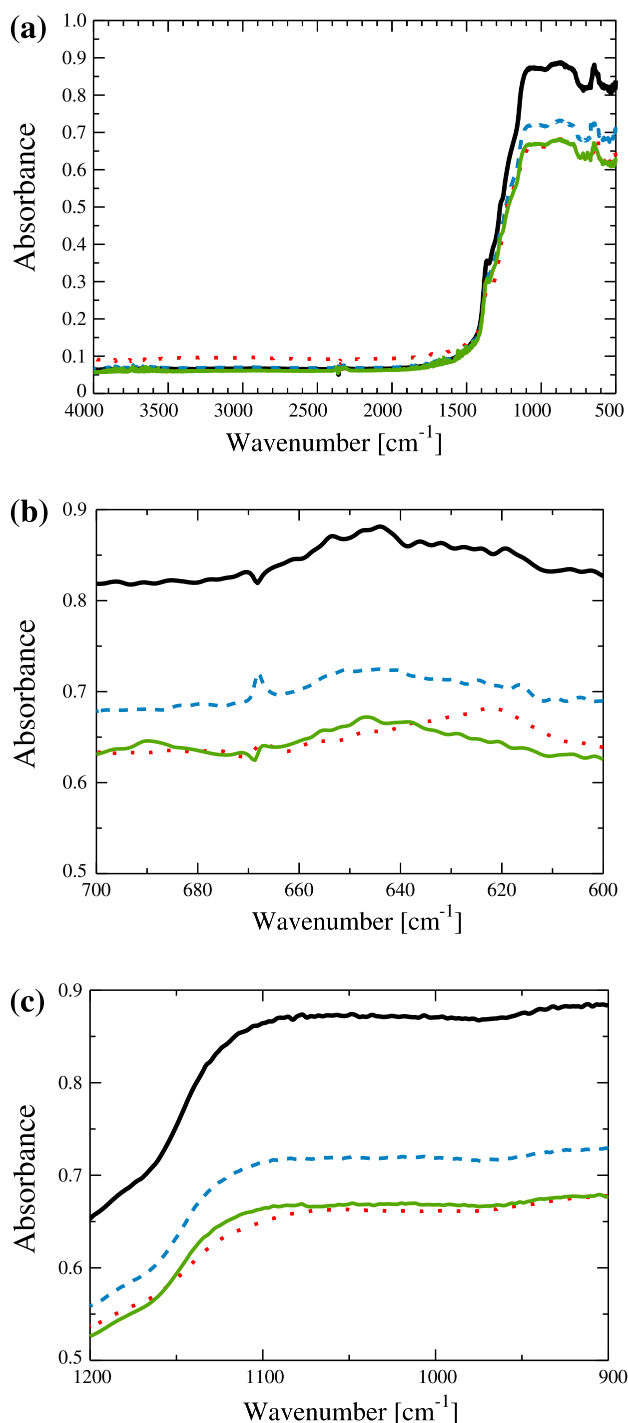

Fig. 2 Temperature-dependent changes in FT-IR spectra measured in the transmission mode: in the whole range of wave numbers (500–400 cm^{-1}; **a**), in the 600–700 cm^{-1} range (**b**), and in the 900–1200 cm^{-1} range (**c**). *Black solid lines*: before, *blue dashed lines*: 1100 °C, *red dotted lines*: 1200 °C, and *green solid lines*: 1300 °C

After the annealing at temperatures above 1250 °C, the apparent color and transparency of the sample changed

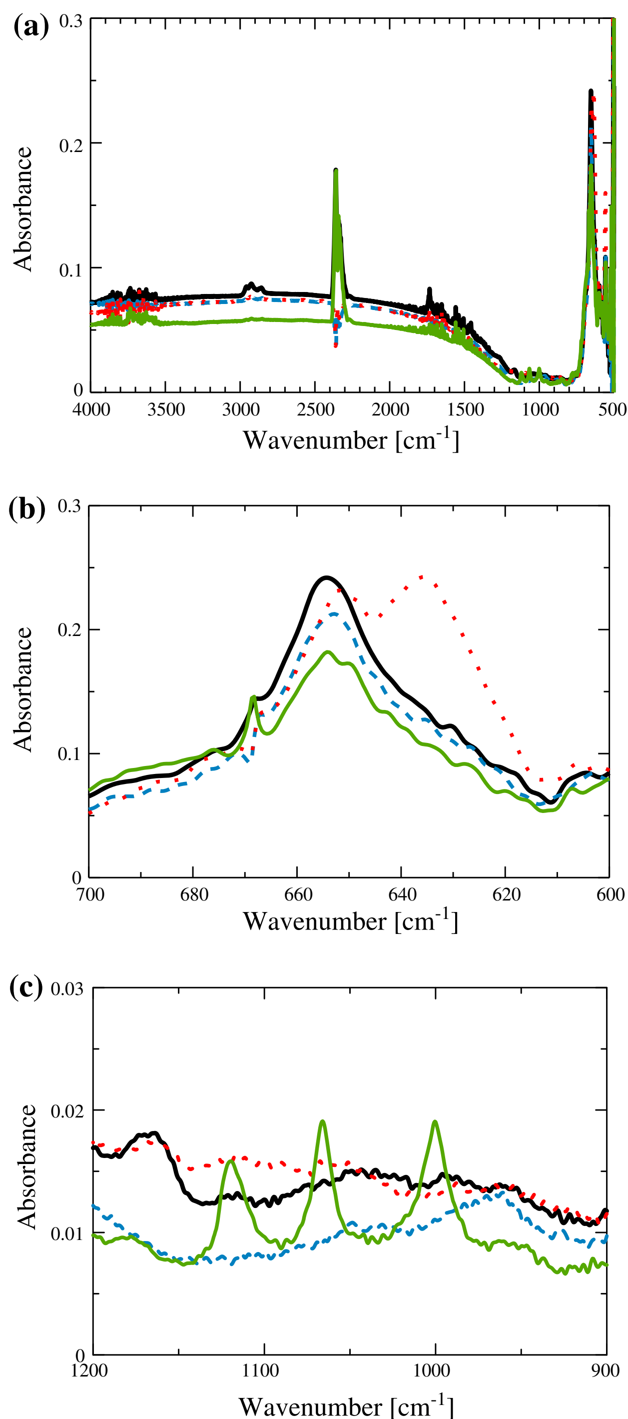

Fig. 3 Temperature-dependent changes in FT-IR spectra measured in the ATR mode: in the whole range of wave numbers (500–400 cm^{-1}; **a**), in the 600–700 cm^{-1} range (**b**), and in the 900–1200 cm^{-1} range (**c**). *Black solid lines*: before, *blue dashed lines*: 1100 °C, *red dotted lines*: 1200 °C, and *green solid lines*: 1300 °C

drastically. That is to say, the surface appeared very dim like ground glass. Furthermore, if the annealing temperature exceeded 1300 °C, the sample became too brittle and easily broken.

In order to show the above-mentioned changes clearly, the surface structure was observed by the laser confocal microscope, and the images obtained are shown in Fig. 4. It is evident that the surface structure starts to change significantly at 1160 °C as shown in Fig. 4c. Complex multiform spots that first appeared on the sample surface at 1160 °C become elliptical, showing the average size of about 20 × 50 μm^2 at 1200 °C (Fig. 4d), and their size and number increase at 1250 °C (e). Furthermore, they seem to gather, converge, and become much larger at 1300 °C (f).

The appearance and growth of elliptical spots quite similar to the cases shown in Fig. 4 can also be confirmed by the ordinary optical microscope as shown in Fig. 5, although the appearance of ellipsoids is difficult to confirm for the annealing at 1160 °C. Interestingly, all the elliptical spots shown in Figs. 4d, e and 5b, c have very similar sizes,

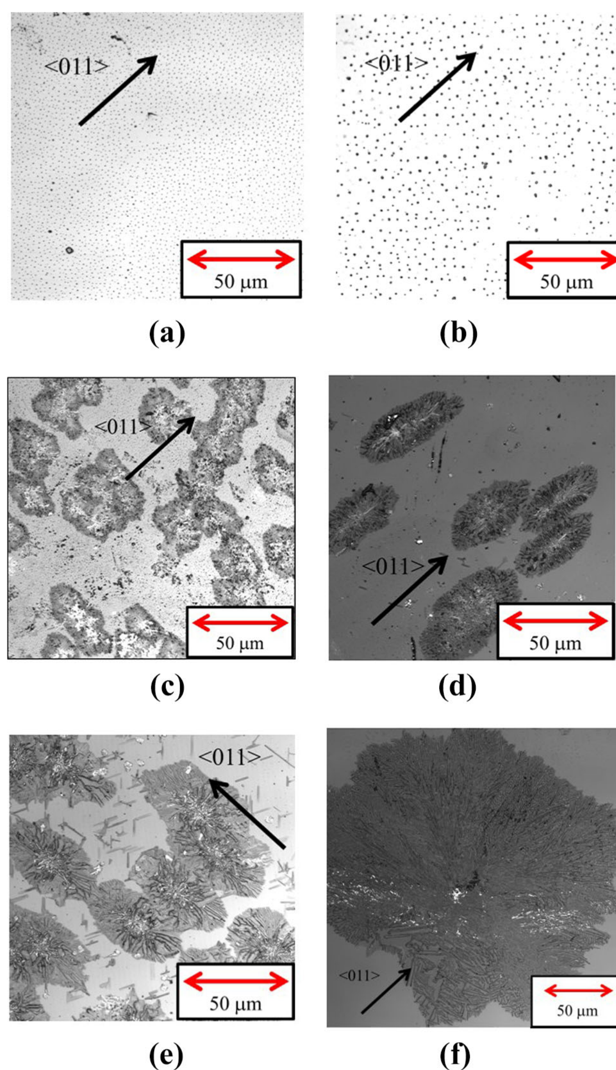

Fig. 4 Temperature-dependent changes in the surface images observed by a laser confocal microscope. **a** before, **b** 1100 °C, **c** 1160 °C, **d** 1200 °C, **e** 1250 °C, **f** 1300 °C

and they are aligned along the <011> axis. This fact indicates that the growth of a certain crystalline structure is related to these spots.

To examine the roughness induced by the thermal annealing, the surface of each sample was observed by the surface profilometer. The change in surface height measured along a straight line with a length of 300 μm is shown in Fig. 6 for the samples before and after the annealing. Note that the ordinate differs in each figure. Furthermore, the average height along each line is shown in Fig. 7 as a function of annealing temperature. In addition, the average and standard deviation of roughness observed by AFM are shown in Fig. 8. It is clearly shown that the surface becomes rough at temperatures above 1160 °C. The roughness is undoubtedly due to the appearance of elliptical spots.

4 Discussion

It has been reported that compounds consisting of Y, Al, and O exhibit the following three crystalline structures. Namely, $YAlO_3$, which is called YAP with a perovskite structure, is the first structure. The second structure, $Y_3Al_5O_{12}$, which is called YAG, takes a garnet structure. The third one is $Y_4Al_2O_9$, which takes a monoclinic structure and is called YAM [25, 26].

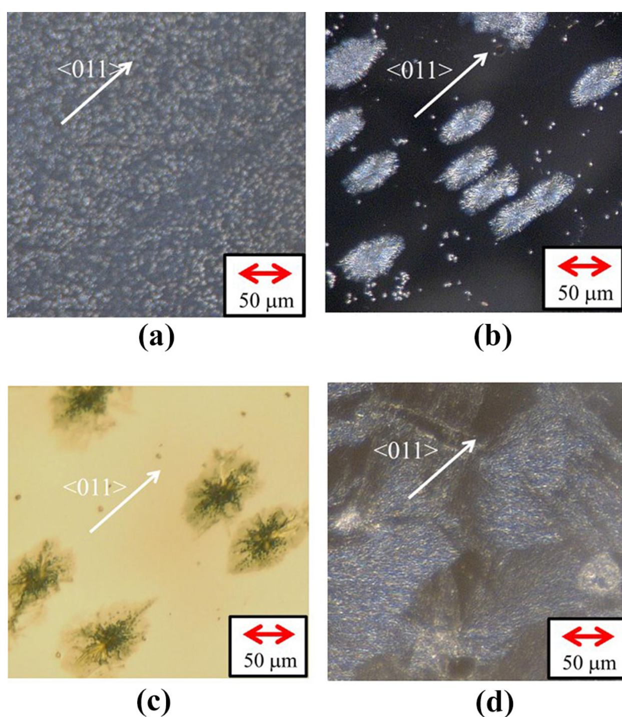

Fig. 5 Surface images of the samples annealed at **a** 1160 °C, **b** 1200 °C, **c** 1250 °C, and **d** 1300 °C observed by an optical microscope. *Note* that apparently different colors of images are simply due to different back lights used for observation

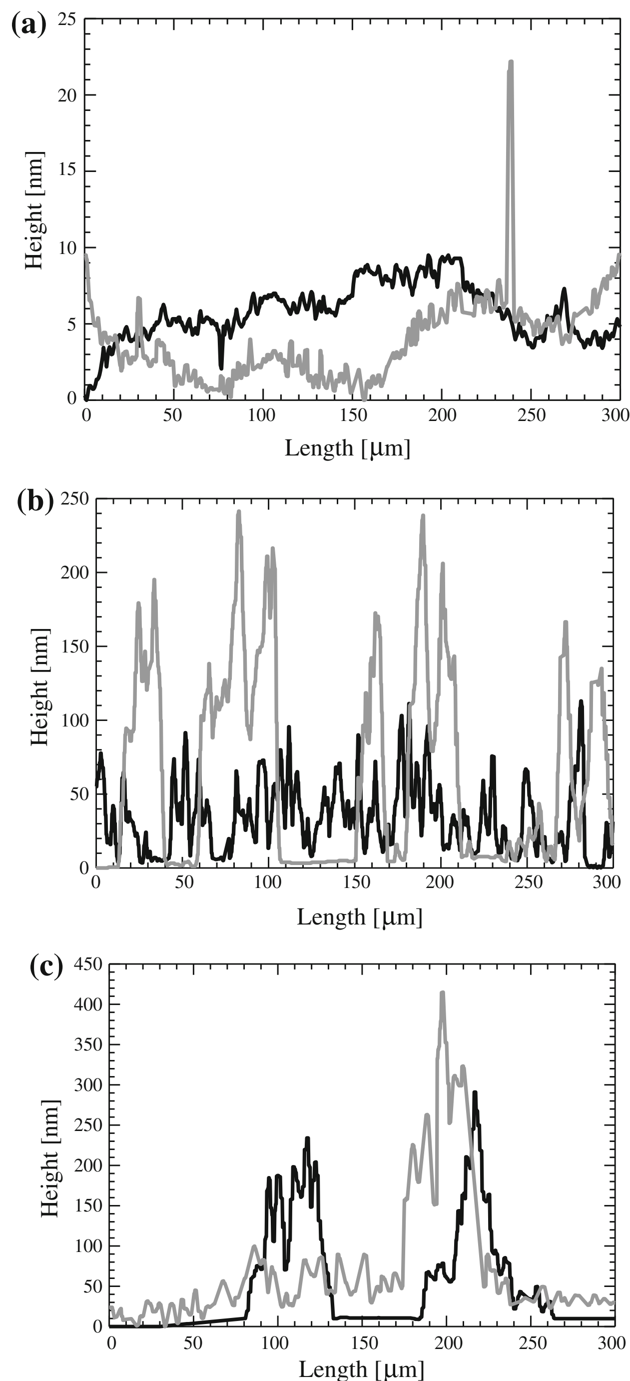

Fig. 6 Position- and temperature-dependent changes in surface roughness observed by a surface profilometer. **a** before (*black*) and at 1100 °C (*gray*), **b** at 1160 °C (*black*) and 1200 °C (*gray*), **c** at 1250 °C (*black*) and 1300 °C (*gray*)

To our knowledge, there have been no papers clarifying the structural changes induced on the surface of single-crystal $YAlO_3$ by thermal annealing. However, as for YAG or $Y_3Al_5O_{12}$, it has been reported that the crystalline $YAlO_3$ and crystalline Al_2O_3 are segregated if YAG is cooled within 5 s to 1375 °C after it was

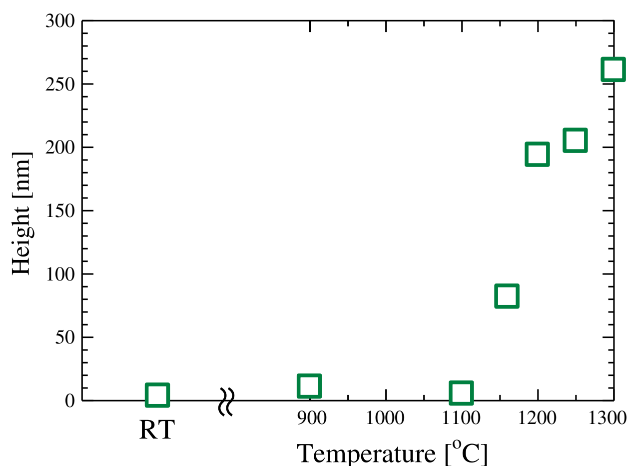

Fig. 7 Average height of the surface roughness observed by the surface profilometer as a function of annealing temperature

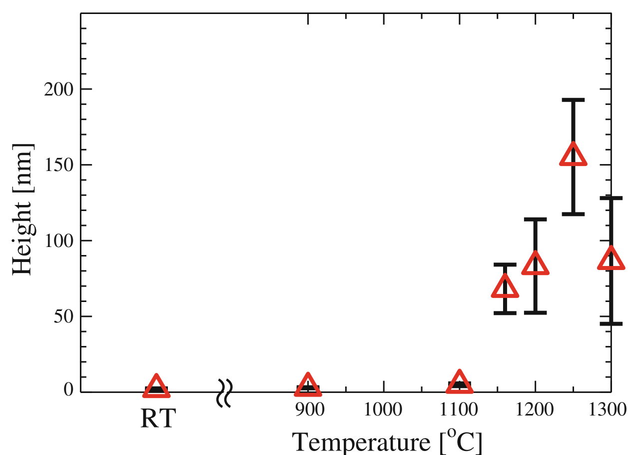

Fig. 8 Changes in the average (*open triangle*) and the standard deviation (I) of the surface height as a function of annealing temperature observed by AFM

annealed at temperatures above its melting point (~1970 °C) [27]. It has also been reported that Al_2O_3 reacts with water vapor at 80 °C to form $Al(OH)_3$ on its surface via AlOOH as an intermediate if it was heated by a microwave oven [21].

Referring to these papers, the above-mentioned results obtained by the present research indicate that the high-temperature annealing induces the following serial structural changes to $YAlO_3$. First, at around 1160 °C, the structure of $YAlO_3$ begins to collapse, forming the structure of YAG via the following two reactions.

$$2YAlO_3 \rightarrow Y_2O_3 + Al_2O_3 \quad (1)$$

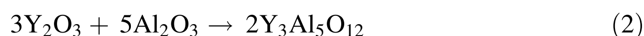

$$3Y_2O_3 + 5Al_2O_3 \rightarrow 2Y_3Al_5O_{12} \quad (2)$$

While the YAG structure becomes stable at 1200 °C, it then segregates to Al_2O_3 and $YAlO_3$ at 1300 °C via the following reaction [27].

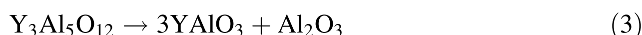

$$Y_3Al_5O_{12} \rightarrow 3YAlO_3 + Al_2O_3 \quad (3)$$

Although the detailed synthesis process of the present samples is unknown, $YAlO_3$ can be synthesized through a chemical reaction of Y_2O_3 and AlOOH [28]. This means that there is a possibility of existence of OH and H in the present $YAlO_3$ samples. This can be a reason for the appearance of OH bonds at 1300 °C. This is consistent with the fact that the intensities of the three IR absorption peaks from 1000 to 1130 cm^{-1} shown in Fig. 3c are small.

The reason for the appearance of the elliptical spots on the sample surface at 1200 and 1250 °C is unknown. However, the spots would have a certain relation with the appearance of the YAG structure, since the two appear and disappear at the respective same temperatures.

All the results obtained in the present work clearly indicate the appearance of YAG at 1160 °C as well as the segregation of YAG and the appearance of OH bonds on the surface at 1300 °C. The findings obtained in the present research are not only crystallographically interesting, but also valuable for semiconductor industries. If thermal annealing is needed in manufacturing semiconductor devices after $YAlO_3$ was deposited, its temperature should be carefully decided by taking the above-mentioned structural changes into account.

5 Conclusion

Perovskite $YAlO_3$ single crystals were thermally annealed at various high temperatures, and the resultant structural changes were examined. As a result, the following serial changes have been clarified.

1. After the annealing at 1160 °C, the crystalline $YAlO_3$ collapses to induce YAG, which coexists with $YAlO_3$ up to 1250 °C.
2. After the annealing at 1200 °C, the $YAlO_3$ structure collapses further to stabilize the YAG structure, and many elliptical spots with a size of about 20 × 50 μm^2 are also induced on the surface.
3. After the annealing at 1300 °C, the YAG structure segregates to Al_2O_3 and $YAlO_3$ and OH bonds appear on the surface.

In situ high-temperature instrumental analyses, such as XRD, FT-IR, and Raman in particular, would be needed for future study.

Acknowledgments Part of this research was supported by Power Academy and JSPS Grant 25-3090 for JSPS Fellows. It was also supported by Research Institute for Science and Engineering, Waseda University, through the ENEOS Research Encouragement Prize and grants from Mitsubishi Materials Corporation and "Early Bird" for young researchers.

References

1. P.G. Neudeck, C. Fazi, IEEE Electron Device Lett. **18**, 96 (1997)
2. T. Egilsson, A. Henry, I.G. Ivanov, J.L. Lindstrom, E. Janzen, Phys. Rev. B **59**, 8008 (1999)
3. J. Hornberger, A.B. Lostetter, K.J. Olejniczak, T. McNutt, S.M. Lal, A. Mantooth, IEEE Aerosp. Conf. Proc. **4**, 2538 (2004)
4. C.M. Johnson, N.G. Wright, M.J. Uren, K.P. Hilton, M. Rahimo, D.A. Hinchley, A.P. Knights, D.J. Morrison, A.B. Horsfall, S. Ortolland, A.G.O. Neill, IEE Proc. Circuits Devices Syst. **148**, 101 (2001)
5. T. Zhao, L. Yang, J. Wang, A.Q. Huang, IEEE Electr. Ship Technol. Symp. 145 (2007)
6. A.K. Agarwal, J.B. Casady, L.B. Rowland, W.F. Valek, M.H. White, C.D. Brandt, IEEE Electron Device Lett. **18**, 586 (1997)
7. Mitsubishi Electric, http://www.mitsubishielectric.com/news/2013/pdf/1225.pdf. Accessed 9 June 2014
8. D.G. Wilk, R.M. Wallace, J.M. Anthony, J. Appl. Phys. **87**, 484 (2000)
9. T. Hosoi, S. Azumo, Y. Kashiwagi, S. Hosaka, R. Nakamura, S. Mitani, Y. Nakano, H. Asahara, T. Nakamura, T. Kimoto, T. Shimura, H. Watanabe, IEEE Int. Electron Devices Meet. **12**, 159 (2012)
10. S.A. Shevlin, A. Curioni, W. Andreoni, Phys. Rev. Lett. **94**, 146401-1 (2005)
11. Y.V. Zorenko, A.S. Voloshinovskii, I.V. Konstankevych, Opt. Spectrosc. **96**, 532 (2004)
12. H. Watanabe, T. Hosoi, T. Kirino, Y. Kagei, Y. Uenishi, A. Chanthaphan, A. Yoshigoe, Y. Teraoka, T. Shimura, Appl. Phys. Lett. **99**, 021907-1 (2011)
13. T. Morimoto, M. Takase, T. Ito, H. Kato, Y. Ohki, Jpn. J. Appl. Phys. **47**, 6858 (2008)
14. E. Hirata, K. Tamagawa, Y. Ohki, Jpn. J. Appl. Phys. **49**, 091102-1 (2010)
15. K. Nomura, S. Okami, X. Xie, M. Mizuno, K. Fukunaga, Y. Ohki, Jpn. J. Appl. Phys. **50**, 021502-1 (2011)
16. D. Yamasaka, K. Tamagawa, Y. Ohki, J. Appl. Phys. **110**, 074103-1 (2011)
17. D. Yamasaka, Y. Horii, T. Morimoto, Y. Ohki, Jpn. J. Appl. Phys. **52**, 071501-1 (2013)
18. T. Morimoto, Y. Horii, T. Inoue, S. Kaneko, M. Harima, Y. Ohki, J. Inst. Eng. Electr. Disch. Jpn. **57**, 3 (2014). (in Japanese)
19. M. Harima, Y. Horii, T. Morimoto, Y. Ohki, IEE Jpn. Proc. Int. Symp. Electr. Insul. Mater. 180 (2014)
20. V. Singh, R.P.S. Chakradhar, J.L. Rao, H.Y. Kwak, Appl. Phys. B **98**, 407 (2010)
21. T. Shirai, M. Yasuoka, K. Watari, Mater. Sci. Eng. B **148**, 221 (2008)
22. S. Mathur, H. Shen, R. Rapalaviciute, A. Kareiva, N. Donia, J. Mater. Chem. **14**, 3259 (2004)
23. K.R. Han, H.J. Koo, C.S. Lim, J. Am. Ceram. Soc. **82**, 1598 (1999)
24. T. Ohwaki, Kobe Steel Engineering Reports **50**, 70 (2000) (in Japanese)
25. S.M. Sim, K.A. Keller, T.I. Mah, J. Mater. Sci. **35**, 713 (2000)
26. J.S. Abell, I.R. Harris, B. Cockayne, B. Lent, J. Mater. Sci. **9**, 527 (1974)
27. M. Gervais, S.L. Floch, N. Gautier, D. Massiot, J.P. Coutures, Mater. Sci. Eng. **45**, 108 (1997)
28. Q. Zhang, F. Saito, Powder Technol. **129**, 86 (2003)